

See discussions, stats, and author profiles for this publication at: <https://www.researchgate.net/publication/236913518>

Synthetic Analogues of the Natural Compound Cryphonectric Acid Interfere with Photosynthetic Machinery through Two Different Mechanisms

ARTICLE in JOURNAL OF AGRICULTURAL AND FOOD CHEMISTRY · MAY 2013

Impact Factor: 2.91 · DOI: 10.1021/jf400698j · Source: PubMed

CITATIONS

5

READS

75

6 AUTHORS, INCLUDING:



[Wagner L Pereira](#)

Universidade Federal de Viçosa (UFV)

8 PUBLICATIONS 26 CITATIONS

[SEE PROFILE](#)



[Deborah Tomaz](#)

Universidade Federal de Viçosa (UFV)

2 PUBLICATIONS 14 CITATIONS

[SEE PROFILE](#)



[Fabrício Marques de Oliveira](#)

Universidade Federal de Viçosa (UFV)

10 PUBLICATIONS 24 CITATIONS

[SEE PROFILE](#)



[Giuseppe Forlani](#)

University of Ferrara

105 PUBLICATIONS 1,486 CITATIONS

[SEE PROFILE](#)

Synthetic Analogues of the Natural Compound Cryphonectric Acid Interfere with Photosynthetic Machinery through Two Different Mechanisms

Róbson Ricardo Teixeira,^{*,†} Wagner Luiz Pereira,[†] Deborah Campos Tomaz,[†] Fabrício Marques de Oliveira,[†] Samuele Giberti,[§] and Giuseppe Forlani^{*,§}

[†]Department of Chemistry, Universidade Federal de Viçosa, Av. P. H. Rolfs S/N, 36.570.000 Viçosa, Minas Gerais, Brazil

[§]Department of Life Science and Biotechnology, University of Ferrara, via L. Borsari 46, 44121 Ferrara, Italy

S Supporting Information

ABSTRACT: A series of isobenzofuran-1(3H)-ones (phthalides), analogues of the naturally occurring phytotoxin cryphonectric acid, were designed, synthesized, and fully characterized by NMR, IR, and MS analyses. Their synthesis was achieved via condensation, aromatization, and acetylation reactions. The measurement of the electron transport chain in spinach chloroplasts showed that several derivatives are capable of interfering with the photosynthetic apparatus. Few of them were found to inhibit the basal rate, but a significant inhibition was brought about only at concentrations exceeding 50 μM . Some other analogues acted as uncouplers or energy transfer inhibitors, with a remarkably higher effectiveness. Isobenzofuranone addition to the culture medium inhibited the growth of the cyanobacterium *Synechococcus elongatus*, with patterns consistent with the effects measured in vitro upon isolated chloroplasts. The most active derivatives, being able to completely suppress algal growth at 20 μM , may represent structures to be exploited for the design of new active ingredients for weed control.

KEYWORDS: isobenzofuran-1(3H)-ones, phthalides, herbicides, photosynthetic electron transport, uncouplers

INTRODUCTION

The world population reached 7 billion people in 2010, and it is projected to grow by 34%, exceeding 9 billion in 2050.¹ One of the challenges to be faced in the 21st century is to produce more food and fiber to feed this increasing population, a goal that in turn demands, among other requirements, the control of various pests and diseases.

With regard to weeds, the use of herbicides is nowadays the most reliable and less expensive tool for weed control. Since the end of World War II, agrochemical companies have produced and commercialized a myriad of herbicides helping farmers to control a broad range of weed species.^{2,3} However, continuous application of products with the same biochemical mechanism of action has led to herbicide resistance.^{4–7} Starting from the 1960s, hundreds of weed biotypes have been reported to survive herbicide application.⁸ As a consequence, there is a constant need for the development of new herbicides to overcome weed resistance. Moreover, modern herbicides should have a favorable combination of properties such as high levels of herbicidal activity, low application rates, crop tolerance, and low toxicity to mammals.

One strategy that can be used in the search and development of new compounds to control weeds is the use of natural products.^{9–18} This strategy has afforded compounds that can be used directly as herbicides.^{19,20} In addition, natural products may serve as lead compounds (prototype bioactive molecules) that can be modified by either semisynthesis or synthesis to afford new active ingredients.^{21,22}

Isobenzofuran-1(3H)-ones (also known as phthalides) represent a class of compounds that have attracted researchers' attention because of their wide range of biological activities,

including antitumoral,²³ anti-HIV,²⁴ anticonvulsant,²⁵ antioxidant,²⁶ and antiplatelet properties²⁷ and the ability to inhibit ATP synthesis in the chloroplast.²⁸ Additionally, these compounds are also valuable synthetic intermediates.^{29,30}

Investigations conducted on a hypovirulent strain of *Cryphonectria parasitica* led to the isolation of several secondary metabolites.³¹ The most abundant compound in EtOAc crude extracts was identified as (4,6-dihydroxy-3-oxo-1,3-dihydroisobenzofuran-1-yl)-3,5-dihydroxybenzoic acid (**1**), also known as cryphonectric acid (Figure 1). A tomato seedling bioassay showed that compound **1** is able to completely inhibit seedling growth at 100 μM ,³¹ but its mode of action was not investigated further.

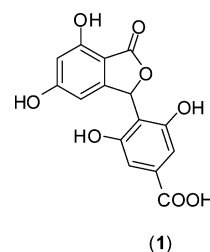


Figure 1. Structure of the naturally occurring isobenzofuran-1(3H)-one cryphonectric acid (**1**).

Received: February 12, 2013

Revised: May 15, 2013

Accepted: May 17, 2013

Published: May 17, 2013

In view of our interest in using natural products as models for the development of new agents to control weeds,^{32–35} we considered cryphonectric acid (**1**) as a model structure and synthesized several analogues for which phytotoxic properties were assessed in vitro on the photosynthetic electron transport chain and in vivo on the growth of the cyanobacterium *Synechococcus elongatus*. To the best of our knowledge, this is the first time that synthetic analogues of compound **1** are shown to interfere with the photosynthetic process. In addition, the distribution of the frontier orbitals HOMO and LUMO, the dipole moment, and the electrostatic potentials for optimized geometries from DFT calculations were determined, and the correlation of the interaction of the molecules with their target sites was attempted. Other physicochemical properties of the evaluated compounds were calculated, and the results are also discussed.

MATERIALS AND METHODS

General Procedures. Analytical grade phthalaldehydic acid, 8-diazabicyclo[5.4.0]undec-7-ene (DBU), cyclohexane-1,3-dione, 5-methylcyclohexane-1,3-dione, 5,5-dimethylcyclohexane-1,3-dione (dime-dione), 5-isopropylcyclohexane-1,3-dione, 1,3-indandione, and dimethylaminopyridine (DMAP) were purchased from Sigma-Aldrich and used without further purification. Mercury(II) acetate, sodium acetate, acetic acid, acetonitrile, and chloroform were purchased from Vetec (Rio de Janeiro, Brazil) and used as received. ¹H and ¹³C NMR spectra were recorded on a Bruker AVANCE DRX 400 spectrometer at 400 and 100 MHz, respectively, using MeOH-*d*₄, CDCl₃, and DMSO-*d*₆ as solvents. Infrared spectra were recorded on a Varian 660-IR, equipped with GladiATR scanning from 4000 to 500 cm^{−1}. HRMS data were recorded under ESI conditions on a micrOTOF-QII Bruker spectrometer. Melting points are uncorrected and were obtained with an MQAPF-301 melting point apparatus (Microquímica, Campinas, Brazil). Analytical thin layer chromatography was carried out on TLC plates recovered with 60GF254 silica gel. Column chromatography was performed over silica gel (60–230 mesh).

Synthesis. 3-(2-Hydroxy-6-oxocyclohexen-1-yl)-3H-isobenzofuran-1-one (**3**). To a 50 mL round-bottom flask were added cyclohexane-1,3-dione (891 mg; 7.95 mmol), acetonitrile (10 mL), and DBU (1.06 mL, 7.10 mmol). The resulting mixture was magnetically stirred for 5 min, after which was added phthalaldehydic acid (**2**) (1070 mg, 7.10 mmol). The reaction mixture was refluxed for 7 h, quenched with 10% HCl (5 mL), and diluted with ethyl acetate (100 mL). The organic layer was separated, washed with water (2 × 20 mL) and brine (10 mL), dried over sodium sulfate, filtered, and concentrated under reduced pressure. Compound **3** was obtained in 64% yield (1121 mg, 4.60 mmol) after recrystallization from ethyl acetate: white solid; TLC *R*_f = 0.20 (ethyl acetate); mp 217.5–218.0 °C; IR (ATR, cm^{−1}) $\bar{\nu}_{\max}$ 2960, 2917, 2887, 2555 (broad band), 1758, 1565, 1380, 1281, 1056, 1025, 944; ¹H NMR (400 MHz, DMSO-*d*₆) δ 1.83–1.91 (m, 2H, H-4'), 2.26–2.45 (m, 4H, H-3'/H-5'), 6.59 (s, 1H, H-3), 7.30 (d, 1H, *J* = 7.6 Hz, H-4), 7.50 (dd, 1H, *J* = 7.6, 7.2 Hz, H-5), 7.65 (dd, 1H, *J* = 7.6, 7.2 Hz, H-6), 7.78 (d, 1H, *J* = 7.6 Hz, H-7); ¹³C NMR (100 MHz, DMSO-*d*₆) δ 20.1 (C-3'/C-5'), 32.6 (C-4'), 74.3 (C-3), 109.1 (C-1'), 121.4 (C-4), 124.2 (C-7), 126.5 (C-8), 128.0 (C-6), 133.6 (C-5), 150.7 (C-9), 170.7 (C-1), 188.0 (C-2'/C-6'). HREIMS *m/z* (*M* + *H*⁺) calcd for C₁₄H₁₃O₄, 245.0814; found, 245.0840.

Compounds **4**, **5**, and **6** were synthesized, respectively, from 4-methylcyclohexa-1,3-dione, 4-isopropyl cyclohexane-1,3-dione, and 1,3-indandione using a procedure similar to that described for the preparation of compound **3**. The structures of compounds **4–6** are supported by the following spectroscopic data.

3-(2-Hydroxy-4-methyl-6-oxocyclohex-1-enyl)isobenzofuran-1(3H)-one (**4**). The compound was obtained as a white solid in 68% yield: TLC *R*_f = 0.50 (ethyl acetate); mp 214.6–218.3 °C; IR (ATR, cm^{−1}) $\bar{\nu}_{\max}$ 2960, 2917, 2886, 2565 (broad band), 1757, 1564, 1380, 1281, 1060, 944, 787, 740, 690, 538; ¹H NMR (400 MHz, MeOH-*d*₄)

δ 1.08 (d, 3H, *J* = 4.8 Hz, −CH₃), 2.13–2.55 (m, 5H, H-4', H-3'/H-5'), 6.69 (s, 1H, H-3), 7.31 (d, 1H, *J* = 7.6 Hz, H-4), 7.49 (dd, 1H, *J* = 7.6, 7.2 Hz, H-5), 7.64 (dd, 1H, *J* = 7.6, 7.2 Hz, H-6), 7.81 (d, 1H, *J* = 7.6 Hz, H-7); ¹³C NMR (100 MHz, MeOH-*d*₄) δ 21.0 (−CH₃), 29.5 (C-3'/C-5'), 42.2 (C-4'), 76.6 (C-3), 110.8 (C-1'), 122.7 (C-4), 125.7 (C-7), 128.2 (C-8), 129.5 (C-6), 135.2 (C-5), 152.4 (C-9), 174.2 (C-1), 189.7 (C-2'/C-6'). HREIMS *m/z* (*M* + *H*⁺) calcd for C₁₅H₁₅O₄, 259.0970; found, 259.0998.

3-(2-Hydroxy-4-isopropyl-6-oxocyclohex-1-enyl)isobenzofuran-1(3H)-one (**5**). The compound was obtained as a white solid in 69% yield: TLC *R*_f = 0.08 (hexane/ethyl acetate 1:3 v/v); mp 176.7–177.8 °C; IR (ATR, cm^{−1}) $\bar{\nu}_{\max}$ 2964, 2872, 2534 (broad band), 2034, 1758, 1555, 1466, 1370, 1341, 1252, 1090, 1063, 950, 727; ¹H NMR (300 MHz, MeOH-*d*₄) δ 0.94 (d, 6H, *J* = 6.9 Hz, −CH(CH₃)₂), 1.57–1.67 (m, 1H, −CH(CH₃)₂), 1.83–1.96 (m, 1H, H-4'), 2.22–2.51 (m, 4H, H-3' and H-5'), 6.68 (s, 1H, H-3), 7.31 (dd, 1H, *J* = 7.5, 0.9 Hz, H-4), 7.50 (t, 1H, *J* = 7.5, H-5), 7.64 (td, 1H, *J* = 7.5, 1.2, H-6), 7.80 (d, 1H, *J* = 7.5, H-7); ¹³C NMR (75 MHz, MeOH-*d*₄) δ 18.7 (−CH(CH₃)₂), 31.7 (−CH(CH₃)₂), 36.8 (C-3'/C-5'), 39.5 (C-4'), 75.3 (C-3), 109.4 (C-1'), 121.4 (C-4), 124.4 (C-7), 126.8 (C-8), 128.2 (C-6), 139.9 (C-5), 151.0 (C-9), 172.9 (C-1), 189.4 (C-2'/C-6'). HREIMS *m/z* (*M* + *H*⁺) calcd for C₁₇H₁₉O₄, 287.1283; found, 287.1260.

2-(3-Oxo-1,3-dihydroisobenzofuran-1-yl)-1H-indene-1,3(2H)-dione (**6**). This substance was obtained as a brown solid in 69% yield: TLC *R*_f = 0.10 (hexane/ethyl acetate 1:1 v/v); mp 214.0–215.3 °C; IR (ATR, cm^{−1}) $\bar{\nu}_{\max}$ 3068, 2922, 1770, 1741, 1702, 1266, 1221, 1054; ¹H NMR (400 MHz, CDCl₃ + DMSO-*d*₆) δ 4.12 (d, 1H, *J* = 2.4 Hz, H-1'), 6.20 (d, 1H, *J* = 2.4 Hz, H-3), 7.84 (m, 8H, H-4, H-5, H-6, H-7, H-3', H-4', H-5', and H-6'); ¹³C NMR δ 55.0 (C-1'), 77.3 (C-3), 124.2 (C-4), 123.1 (C-3'), 123.6 (C-6'), 125.3 (C-7), 125.8 (C-6), 129.5 (C-8), 134.4 (C-4'/C-5'), 136.1 (C-5), 142.1 (C-8'), 142.5 (C-9'), 147.4 (C-9), 169.4 (C-1), 194.9 (C-2'), 196.3 (C-7'). HREIMS *m/z* (*M* + *H*⁺) calcd for C₁₇H₁₁O₄, 279.0657; found, 279.0665.

3-(2-Hydroxy-4,4-dimethyl-6-oxocyclohexen-1-yl)isobenzofuran-1(3H)-one (**7**). To a 25 mL round-bottom flask were added dime-dione (500 mg; 3.57 mmol), chloroform (5 mL), and DBU (0.53 mL, 3.57 mmol). The resulting mixture was stirred under nitrogen atmosphere for 5 min, after which phthalaldehydic acid (**2**) was added (495 mg, 3.30 mmol). The reaction mixture was stirred at room temperature for 5 h, quenched with 10% HCl (5 mL), and diluted with ethyl acetate (100 mL). The organic layer was separated, washed with water (2 × 20 mL) and brine (10 mL), dried over sodium sulfate, filtered, and concentrated under reduced pressure. Compound **7** was obtained in 95% yield (850 mg, 3.12 mmol) after recrystallization from ethyl acetate: white solid; TLC *R*_f = 0.10 (hexane/ethyl acetate 1:1 v/v); mp 212.1–213.0 °C; IR (ATR, cm^{−1}) $\bar{\nu}_{\max}$ 2200–3000 (broad band, OH), 2960, 2933, 2885, 1763, 1569, 1382, 1321, 1284, 1059, 942, 789, 738, 694, 613, 574; ¹H NMR (400 MHz, MeOH-*d*₄) δ 1.09 (s, 6H, 2 × CH₃), 2.35 (s, 4H, H-3'/H-5'), 6.70 (s, 1H, H-3), 7.31 (d, 1H, *J* = 7.6 Hz, H-4), 7.50 (t, 1H, *J* = 7.6 Hz, H-5), 7.66 (t, 1H, *J* = 7.6 Hz, H-6), 7.81 (d, 1H, *J* = 7.6 Hz, H-7); ¹³C NMR (100 MHz, MeOH-*d*₄) δ 28.5 (−CH₃), 33.1 (C-4'), 47.9 (C-3'/C-5'), 76.6 (C-3), 110.1 (C-1'), 122.6 (C-4), 125.8 (C-7), 128.2 (C-8), 129.5 (C-6), 135.2 (C-5), 152.4 (C-9), 174.2 (C-1), 188.9 (C-2'/C-6'). HREIMS *m/z* (*M* + *H*⁺) calcd for C₁₆H₁₇O₄, 273.1127; found, 273.1124.

3-(2,6-Dihydroxyphenyl)isobenzofuran-1(3H) one (**8**). A 50 mL round-bottom flask was charged with compound **3** (477 mg, 1.95 mmol), acetic acid (20 mL), Hg(OAc)₂ (1897 mg; 5.93 mmol), and NaOAc (481 mg, 5.86 mmol). The resulting mixture was stirred and refluxed for 5 h. After this time, the reaction mixture was cooled, 5 mL of 1 mol L^{−1} HCl was added, and the mixture was stirred for an additional 15 min. The mixture was filtered through a pad of Celite and the filtrate diluted with ethyl acetate (60 mL). The organic layer was separated, washed with saturated sodium bicarbonate aqueous solution (2 × 10 mL), water (5 mL), brine (5 mL), and 0.200 mol L^{−1} sodium EDTA aqueous solution (2 × 15 mL). After that, the organic layer was dried over sodium sulfate, filtered, and concentrated under reduced pressure. The residue was purified by silica gel column chromatography (hexane/ethyl acetate 1:3 v/v). This procedure afforded compound **8** in 68% yield (320 mg; 1.32 mmol): white solid;

TLC R_f = 0.70 (hexane/ethyl acetate 1:3 v/v); mp 238.6–239.8 °C; IR (ATR, cm^{-1}) $\bar{\nu}_{\text{max}}$ 3470, 3296 (broad bands), 1712, 1469, 1011, 945, 715; ^1H NMR (400 MHz, CDCl_3 + $\text{DMSO}-d_6$) δ 6.29 (d, 2H, J = 8.0 Hz, H-3'/H-5'), 6.92 (t, 1H, J = 8.0 Hz, H-4'), 7.02 (s, 1H, H-3), 7.31 (d, 1H, J = 7.2 Hz, H-4), 7.47 (t, 1H, J = 7.6 Hz, H-6), 7.59 (t, 1H, J = 7.2 Hz, H-5), 7.81 (d, 1H, J = 7.6 Hz, H-7); ^{13}C NMR (100 MHz, CDCl_3 + $\text{DMSO}-d_6$) δ 75.6 (C-3), 106.9 (C-3'/C-5'), 108.6 (C-1'), 121.8 (C-4), 124.2 (C-7), 127.2 (C-8), 127.9 (C-6), 130.2 (C-4'), 133.3 (C-5), 151.1 (C-9), 157.5 (C-2'/C-6'), 171.5 (C-1). HREIMS m/z ($M + H^+$): calcd for $\text{C}_{14}\text{H}_{11}\text{O}_4$, 243.0657; found, 243.0658.

Isobenzofuranones **9** and **10** were obtained, respectively, from chemicals **4** and **5** using a procedure similar to that described for the preparation of compound **8**. Structures of **9** and **10** are supported by the following data.

3-(2,6-Dihydroxy-4-methylphenyl)isobenzofuran-1(3H)-one (9). The compound was obtained as a pale yellow solid via aromatization of compound **4** in 71% yield (purified by silica gel column chromatography, using hexane/ethyl acetate 1:3 v/v as the eluting solvent): TLC R_f = 0.82 (hexane/ethyl acetate 1:3 v/v); mp 228–231 °C; IR (ATR, cm^{-1}) $\bar{\nu}_{\text{max}}$ 3579, 3201 (broad band), 2924, 2853, 1721, 1618, 1595, 1305, 1046, 952, 821, 734, 684, 535; ^1H RMN (200 MHz, CDCl_3 + $\text{MeOH}-d_4$) δ 1.94 (s, 3H, $-\text{CH}_3$), 5.94 (s, 2H, H-3'/H-5'), 6.82 (s, 1H, H-3), 7.11 (d, 1H, J = 7.2 Hz, H-4), 7.16–7.44 (m, 2H, H-5 and H-6), 7.62 (d, 1H, J = 7.2 Hz, H-7); ^{13}C NMR (50 MHz, CDCl_3 + $\text{MeOH}-d_4$) δ 22.5 ($-\text{CH}_3$), 72.2 (C-3), 106.9 (C-1'), 109.1 (C-3'/C-5'), 123.2 (C-4), 125.4 (C-6), 128.5 (C-8), 128.9 (C-7), 134.4 (C-5), 141.9 (C-4'), 152.6 (C-9), 158.3 (C-2'/C-6'), 173.2 (C-1). HREIMS m/z ($M + H^+$): calcd for $\text{C}_{15}\text{H}_{13}\text{O}_4$, 257.0814; found, 257.0880.

3-(2,6-Dihydroxy-4-isopropylphenyl)isobenzofuran-1(3H)-one (10). The compound was obtained as a viscous orange oil via aromatization of compound **5** in 94% yield (purified by silica gel column chromatography, using hexane/ethyl acetate 1:1 v/v as the eluting solvent): TLC R_f = 0.44 (hexane/ethyl acetate 1:1 v/v); IR (ATR, cm^{-1}) $\bar{\nu}_{\text{max}}$ 3305 (broad band), 2959, 2924, 2870, 2159, 1726, 1621, 1596, 1433, 1034, 732; ^1H NMR (300 MHz, $\text{MeOH}-d_4$) δ 1.17 (d, 6H, J = 6.9 Hz, $-\text{CH}(\text{CH}_3)_2$), 2.68 (sept, 1H, J = 6.9 Hz, $-\text{CH}(\text{CH}_3)_2$), 6.17 (s, 2H, H-3'/H-5'), 7.02 (s, 1H, H-3), 7.30 (dd, 1H, J = 7.5, J = 0.9 Hz, H-4), 7.49 (t, 1H, J = 7.2 Hz, H-5), 7.63 (td, 1H, J = 7.5, 1.2 Hz, H-6), 7.82 (d, 1H, J = 7.5 Hz, H-7); ^{13}C NMR (75 MHz, $\text{MeOH}-d_4$) δ 22.9 ($-\text{CH}(\text{CH}_3)_2$), 34.2 ($-\text{CH}(\text{CH}_3)_2$), 76.8 (C-3), 104.6 (C-3'/C-5'), 105.8 (C-1'), 121.8 (C-4), 124.1 (C-6), 127.0 (C-8), 128.0 (C-7), 133.7 (C-5), 151.8 (C-9), 152.3 (C-4'), 157.6 (C-2'/C-6'), 173.4 (C-1). HREIMS m/z ($M + H^+$): calcd for $\text{C}_{17}\text{H}_{17}\text{O}_4$, 285.1127; found, 285.1116.

3-Oxo-1,3-dihydroisobenzofuran-1-yl)-1,3-phenylene diacetate (11). A round-bottom flask (25 mL) was charged with compound **8** (0.109 g, 0.45 mmol), chloroform (5 mL), acetic anhydride (0.16 mL, 1.62 mmol), and a catalytic amount of DMAP (0.005 g, 0.045 mmol). The reaction mixture was stirred at room temperature for 12 h. The solvent was removed, and compound **11** was purified by recrystallization from ethyl acetate, affording a white solid in 44% yield (0.064 g, 0.20 mmol). The structure of the compound is supported by the following data: TLC R_f = 0.54 (hexane/ethyl acetate 1:1 v/v); mp 175.9–177.8 °C; IR (ATR, cm^{-1}) $\bar{\nu}_{\text{max}}$ 1756, 1611, 1465, 1369, 1285, 1170, 1023, 975; ^1H NMR (200 MHz, $\text{DMSO}-d_6$) δ 2.01 (brs, 6H, $2 \times -\text{COCH}_3$), 6.85 (s, 1H, H-3), 7.08 (d, 2H, J = 8.2 Hz, H-3'/H-5'), 7.25 (d, 1H, J = 6.8 Hz, H-4), 7.53 (t, 1H, J = 8.2 Hz, H-4'), 7.58–7.75 (m, 2H, H-5 and H-6), 7.95 (d, 1H, J = 7.4 Hz, H-7); ^{13}C NMR (50 MHz, DMSO) δ 22.0 ($-\text{COCH}_3$), 76.0 (C-3), 122.3 (C-3'/C-5'), 123.2 (C-1'), 124.4 (C-4), 126.6 (C-7), 127.3 (C-8), 131.2 (C-6), 132.5 (C-4'), 136.5 (C-5), 150.67 (C-9), 151.61 (C-2'/C-6'), 170.5 (C-1), 172.0 ($-\text{COCH}_3$). HREIMS m/z ($M + H^+$): calcd for $\text{C}_{18}\text{H}_{15}\text{O}_6$, 327.0869; found, 327.0848.

Using compounds **9** and **10**, respectively, as starting materials, acetylated derivatives **12** and **13** were obtained using a procedure similar to that described for the preparation of compound **11**. Structures of **12** and **13** are supported by the following data.

5-Methyl-2-(3-oxo-1,3-dihydroisobenzofuran-1-yl)-1,3-phenylene diacetate (12). The compound was obtained as a pale yellow solid

from compound **9** in 93% yield (after purification by silica gel column chromatography, using hexane/ethyl acetate 1:2 v/v as the eluting solvent): TLC R_f = 0.8 (hexane/ethyl acetate 1:2 v/v); mp 171.5–172.3 °C; IR (ATR, cm^{-1}) $\bar{\nu}_{\text{max}}$ 2925, 2855, 1758, 1621, 1172, 1040, 974, 692, 738; ^1H NMR (200 MHz, $\text{DMSO}-d_6$) δ 1.99 (brs, 6H, $2 \times -\text{COCH}_3$), 2.31 (s, 3H, CH_3), 6.78 (s, 1H, H-3), 6.94 (s, 2H, H-3'/H-5'), 7.23 (d, 1H, J = 7.4 Hz, H-4), 7.61 (dd, 1H, J = 7.4, 7.2 Hz, H-5), 7.73 (dd, 1H, J = 7.4, 7.2 Hz, H-6), 7.93 (d, 1H, J = 7.2 Hz, H-7); ^{13}C NMR (50 MHz, $\text{DMSO}-d_6$) δ 22.0 ($-\text{COCH}_3$), 22.3 ($-\text{CH}_3$), 76.0 (C-3), 119.3 (C-3'/C-5'), 123.6 (C-1'), 124.4 (C-4), 126.5 (C-6), 127.3 (C-8), 131.0 (C-7), 136.4 (C-5), 142.9 (C-9'), 150.8 (C-4'), 151.4 (C-2'/C-6'), 170.5 (C-1), 171.9 ($-\text{COCH}_3$). HREIMS m/z ($M + H^+$): calcd for $\text{C}_{19}\text{H}_{17}\text{O}_6$, 341.1025; found, 341.1030.

5-Isopropyl-2-(3-oxo-1,3-dihydroisobenzofuran-1-yl)-1,3-phenylene diacetate (13). This compound was obtained as a solid in 78% yield (after purification by recrystallization from ethyl acetate) from compound **10**: TLC R_f = 0.81 (hexane/ethyl acetate 1:1 v/v); mp 157.5–158.1 °C; IR (ATR, cm^{-1}) $\bar{\nu}_{\text{max}}$ 2963, 2930, 2870, 1756, 1620, 1366, 1288, 1179, 1030, 973, 739, 562; ^1H NMR (200 MHz, $\text{DMSO}-d_6$) δ 1.16 (d, 1H, J = 7.0 Hz, $-\text{CH}(\text{CH}_3)_2$), 1.98 (brs, 6H, $2 \times -\text{COCH}_3$), 2.89 (sept, 1H, J = 7.0 Hz, $-\text{CH}(\text{CH}_3)_2$), 6.78 (s, 1H, H-3), 7.00 (s, 2H, H-3'/H-5'), 7.26 (d, 1H, J = 7.2 Hz, H-4), 7.54–7.78 (m, 2H, H-5 and H-6), 7.93 (d, 1H, J = 7.2 Hz, H-7); ^{13}C NMR (50 MHz, $\text{DMSO}-d_6$) δ 22.0 ($-\text{COCH}_3$), 25.0 ($-\text{CH}(\text{CH}_3)_2$), 34.8 ($-\text{CH}(\text{CH}_3)_2$), 76.0 (C-3), 119.6 (C-3'/C-5'), 121.0 (C-1'), 124.5 (C-4), 126.5 (C-6), 127.3 (C-8), 131.1 (C-7), 136.4 (C-5), 150.7 (C-9), 151.5 (C-2'/C-6'), 153.9 (C-4'), 170.5 (C-1), 171.9 ($-\text{COCH}_3$). HREIMS m/z ($M + H^+$): calcd for $\text{C}_{21}\text{H}_{21}\text{O}_6$, 369.1338; found, 369.1418.

Biological Assays. Photosynthetically active thylakoid membranes were isolated from market spinach (*Spinacia oleracea* L.) leaves, as previously described.³⁶ Briefly, 20 g of deveined plant material was resuspended in 100 mL of ice-cold 20 mM Tricine/NaOH buffer (pH 8.0), containing 10 mM NaCl, 5 mM MgCl_2 , and 0.4 M sucrose, and homogenized for 30 s in a blender at maximal speed. The homogenate was filtered through surgical gauze, and the filtrate was centrifuged at 4 °C for 1 min at 500g; the supernatant was further centrifuged for 10 min at 1500g. Pelleted chloroplasts were osmotically swollen by resuspension in sucrose-lacking buffer, immediately diluted 1:1 with sucrose-containing buffer, and kept on ice in the dark until used. Following dilution with 80% (v/v) acetone, the chlorophyll content was calculated on the basis of Arnon's formula. The basal rate of photosynthetic electron transport was measured following light-driven ferricyanide reduction. Aliquots of membrane preparations corresponding to 15 μg of chlorophyll were incubated at 24 °C in 1 mL cuvettes containing 20 mM Tricine/NaOH buffer (pH 8.0), 10 mM NaCl, 5 mM MgCl_2 , 0.2 M sucrose/ and 1 mM $\text{K}_3[\text{Fe}(\text{CN})_6]$. The assay was initiated by exposure to saturating light (800 $\mu\text{mol m}^{-2} \text{s}^{-1}$), and the rate of ferricyanide reduction was measured at 1 min intervals for 20 min in a GE Healthcare Novaspec Plus spectrophotometer at 420 nm against an exact blank. Activity was calculated over the linear portion of the curve from a molar extinction coefficient of 1000 $\text{M}^{-1} \text{cm}^{-1}$. Isobenzofuranones **3**–**13** were dissolved in DMSO so as to obtain 20 mM solutions that were then water diluted, as appropriate. Their effect upon the photosynthetic electron transport was evaluated in parallel assays in which the compounds were added to the reaction mixture to a final concentration ranging from 0.1 to 200 μM . For each dose, the assay was carried out at least in triplicate, and results were expressed as percentage of untreated controls. Reported values are means \pm SE over replicates. The concentrations causing 50% inhibition (IC_{50}) and their confidence limits were estimated by nonlinear regression analysis using Prism 5 for Windows, version 5.01 (GraphPad Software).

S. elongatus, strain PCC 6301, was grown at 24 ± 1 °C under 14 h days (150 $\mu\text{mol m}^{-2} \text{s}^{-1}$ PAR) and 10 h nights in 250 mL Erlenmeyer flasks containing 60 mL of ATCC minimal medium 616 (Bg11; <http://www.lgcstandards-atcc.org/Attachments/3868.pdf>). Subcultures were made every 4 weeks by transferring 10 mL aliquots to 50 mL of fresh medium. Growth was followed by measuring chlorophyll concentration. Culture aliquots (0.5–1.0 mL) were withdrawn, and

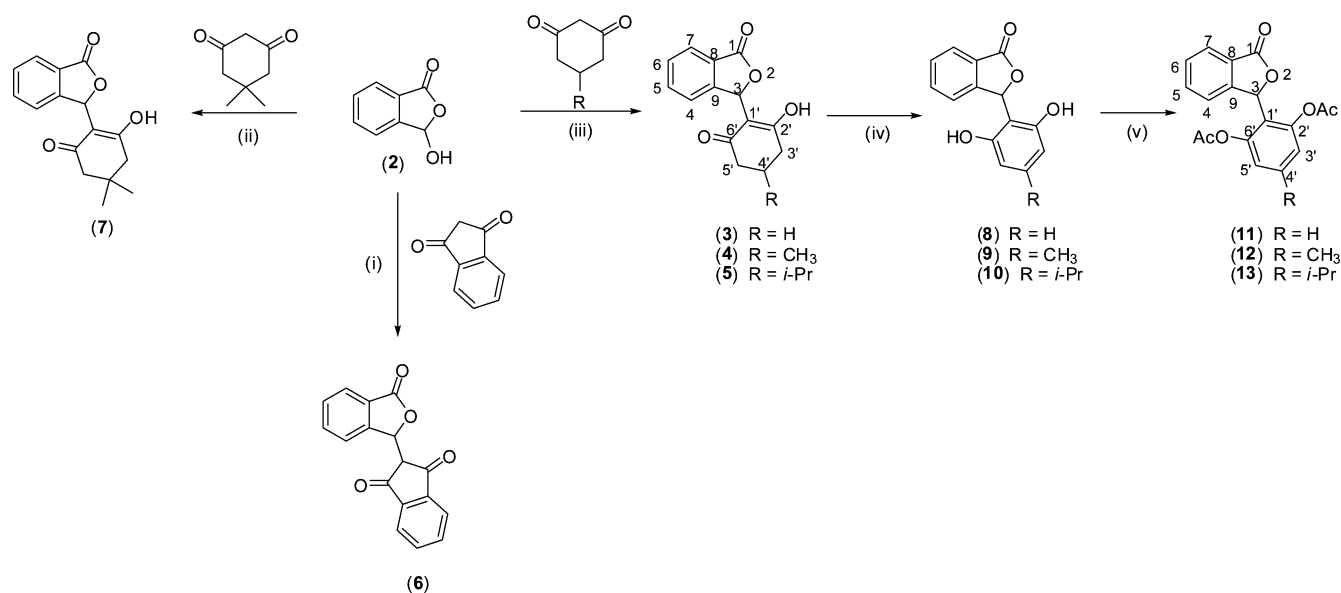


Figure 2. Synthesis of compounds 3–13.

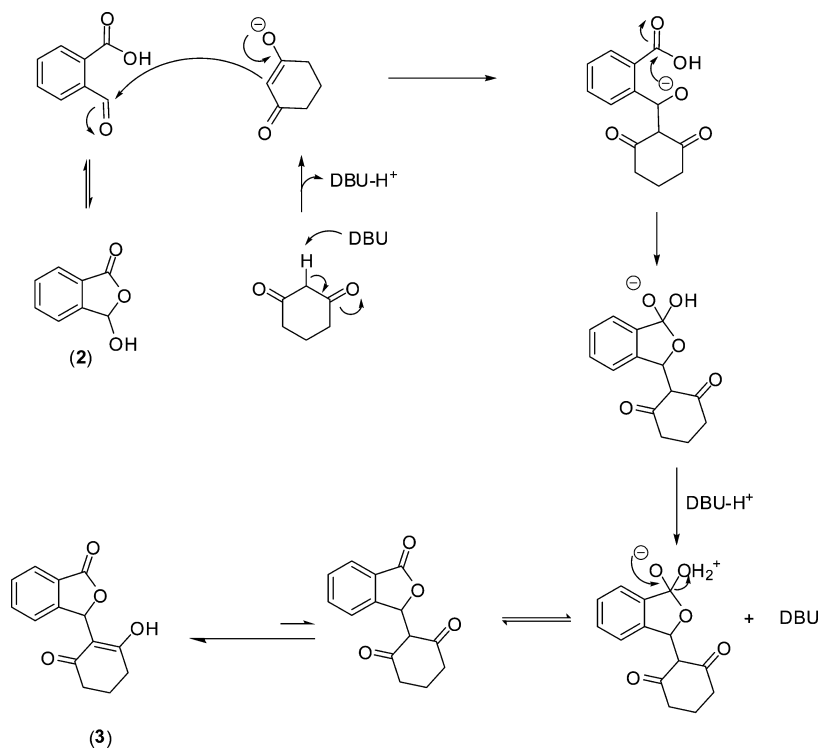


Figure 3. Proposed mechanism for the formation of compound 3.

cells were sedimented by centrifugation for 3 min at 14000g. Pellets were resuspended with 1.0 mL of methanol, and solubilization was allowed to proceed for 30 min in the dark, with occasional mixing. Samples were then centrifuged again, and total chlorophyll content in the supernatant was estimated spectrophotometrically, as described.³⁷ Following logarithmic transformation of data, growth constants and generation times were calculated from the linear portion of each curve.

Late log-grown cells were sedimented by centrifugation 5 min at 4000g and used to inoculate 25-well squared Petri dishes, 4.0 mL per well, to an initial density of 2.0 mg L⁻¹ chlorophyll. Suitable dilutions in Bg11 medium of a 20 mM stock solution of a given compound in DMSO were added so as to obtain concentrations ranging from 5 to 100 μ M. A complete randomized design with four replications was adopted. Cell growth in each well was followed for 1 week by daily

destructive harvest, as indicated. Following logarithmic transformation of data, growth constants were calculated and expressed as percent of the mean value for untreated controls. Means \pm SE over replicates are reported.

Quantum Chemical and Physicochemical Parameter Calculations. Physicochemical parameters were calculated using the software provided by Molinspiration Cheminformatics (Bratislava, Slovak Republic, www.molinspiration.com). Molecular attributes analyzed were *n*-octanol/water partition coefficient (cLogP), the amount of hydrogen bond donors (HBD), the amount of hydrogen bond acceptor (HBA), the molecular weight of the compounds (MW), the number of rotatable bonds (nRotb), and polar surface area (PSA). The numbers of hydrogen bond donors and hydrogen bond acceptors were calculated as described by Lipinski and co-workers.³⁸ The

calculation of the molecule's PSA was performed by the aforementioned software using the method of Ertl and coauthors.³⁹

Molecular modeling and DFT calculations for compounds 3–13 were performed using Spartan 10 and Gaussian 09 programs.^{40,41} Semiempirical computational geometry optimizations were carried out with the Spartan 10 software package employing the semiempirical PM6 method. Next, the optimization was held for the lowest energy conformation identified in each case. The outputs obtained with the Spartan 10 program (reported in the Supporting Information) were utilized to generate inputs for the calculations with the Gaussian 09 program. Lowest energy conformers were optimized in the gas phase at the B3LYP/6-311++G(2d,p) level of theory, where B3LYP is the Becke's three-parameter hybrid functional using the Lee–Yang–Parr correlation functional.⁴² The DFT/B3LYP method is recommended for the estimation of molecular properties related to reactivity of molecules, such as the energy of the highest occupied molecular orbital (E_{HOMO}) and the energy of the lowest unoccupied molecular orbital (E_{LUMO}).⁴³ DFT energy calculations (B3LYP/6-311++G(2d,p)) afforded predictions of the HOMO–LUMO energies and dipole moment. In this case, considerations in terms of solvent effects on geometries and relative conformational stabilities have been taken using the SMD solvation model and water as solvent.⁴⁴ Electrostatic potentials and HOMO/LUMO maps (Supporting Information Figure S1) were calculated for the geometries that resulted from DFT calculations using Gaussian 09 and GaussView 5 at B3LYP/6-311++G(2d,p).

RESULTS AND DISCUSSION

Synthesis of Isobenzofuran-1(3H)-ones. The isobenzofuran-1(3H)-ones, structurally similar to the secondary metabolite 1 (Figure 1), were prepared as outlined in Figure 2.

DBU-promoted condensation reactions between the commercially available phthalaldehydic acid (2) and appropriate cyclic 1,3-diketones gave the compounds 3–7 in yields ranging from 64 to 95%.^{45,46} With compound 3 as an example, formation of isobenzofuranones mediated by DBU can be envisioned as proposed in Figure 3.

Aromatization of phthalides 3–7 promoted by $\text{Hg}(\text{OAc})_2/\text{NaOAc}$ gave the phenol derivatives 8–10 (Figure 3).⁴⁷ Finally, straightforward acetylation of chemicals 8–10 in the presence of DMAP afforded substances 11–13. All of the compounds were fully characterized by IR and NMR spectroscopy, as well as mass spectrometry. HSQC and HMBC experiments allowed establishment of the hydrogen and carbon assignments.

Biological Activity of Isobenzofuran-1(3H)-ones. Previous studies showing that some isobenzofuran-1(3H)-ones are capable of interfering with ATP synthesis in the chloroplast²⁸ prompted us to investigate the effect of compounds 3–13 on the chloroplastic electron transport chain, measured as the light-driven reduction of potassium ferricyanide by isolated thylakoid membranes. The results are summarized in Table 1. Indeed, several compounds were found to affect the Hill reaction. Three cryphonectric acid analogues mildly to moderately inhibited ferricyanide reduction, with a 50% reduction of the electron transport rate in the range from 0.1 to 1 mM (IC_{50} of 170 ± 7 , 219 ± 31 , and $750 \pm 360 \mu\text{M}$ for compounds 7, 8, and 13, respectively). On the contrary, four other compounds (9, 10, 11, and 12) caused an apparent stimulation of the electron transport chain.

The latter effect was more pronounced and was still evident in the 10^{-6} – 10^{-5} M range (Figure 4). An increase in the rate of ferricyanide reduction by isolated thylakoids may depend upon a partial dissipation of the proton gradient across the membrane, which in turn can be caused by the presence of uncouplers. Substances such as ammonia, some organic acids,

Table 1. In Vitro Effects of Compounds 3–13 on Ferricyanide Reduction by Chloroplasts Isolated from *S. oleracea* Leaves^a

compd	50 $\mu\text{mol L}^{-1}$	100 $\mu\text{mol L}^{-1}$	200 $\mu\text{mol L}^{-1}$
3	99.2 ± 1.6	114.1 ± 1.5	104.7 ± 1.3
4	102.7 ± 0.3	96.5 ± 2.0	93.8 ± 3.2
5	93.2 ± 0.5	92.0 ± 2.8	97.5 ± 2.8
6	108.6 ± 0.5	105.0 ± 3.4	78.2 ± 4.3
7	86.1 ± 0.0	68.0 ± 1.4	44.2 ± 0.2
8	90.2 ± 0.1	92.4 ± 1.3	55.7 ± 3.0
9	133.5 ± 2.0	125.6 ± 0.8	116.1 ± 4.5
10	185.7 ± 2.4	156.7 ± 4.9	87.1 ± 2.5
11	218.3 ± 4.0	222.5 ± 1.1	189.9 ± 0.9
12	201.9 ± 3.7	192.4 ± 5.9	161.1 ± 6.5
13	92.0 ± 1.5	83.1 ± 1.3	75.9 ± 1.6

^aBasal activity was measured either in the absence or in the presence of a given compound at increasing concentration, as indicated. Values were expressed as percentage of untreated controls ($46.9 \pm 3.0 \text{ nmol ferricyanide reduced s}^{-1} \text{ mg}^{-1} \text{ chlorophyll}$) and are means \pm SE over at least three replicates.

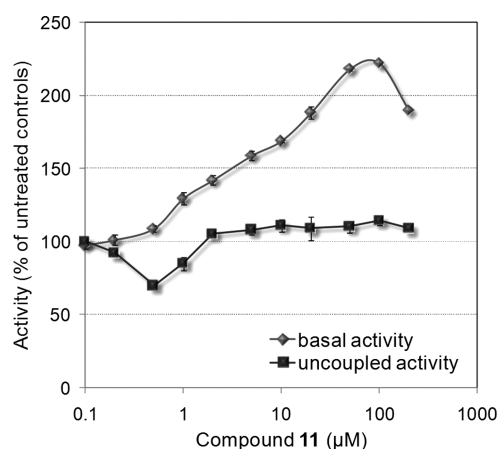


Figure 4. Effects of compound 11 on the Hill reaction under basal and uncoupling conditions. Ferricyanide reduction by isolated spinach chloroplasts was measured in the presence of increasing concentrations of the analogue. Results were expressed as percentage values with respect to untreated controls and are means \pm SE over at least three replicates. Uncoupling conditions were obtained by adding 2 mM NH_4Cl to the reaction mixture. Activity levels for untreated controls were 48.2 ± 2.7 and $150.8 \pm 4.1 \text{ nmol ferricyanide reduced s}^{-1} \text{ mg}^{-1} \text{ chlorophyll}$ under basal and uncoupled conditions, respectively.

and phenols are able to act as proton shuttles: because it requires the creation and the maintenance of a proton gradient between the lumen and the stroma of the chloroplast, photosynthesis is affected by any compound that makes the membrane permeable to protons. As a consequence, ATP synthesis is impaired. Alternatively, the same effect can result from the inhibition of the energy transfer through an interaction with the coupling factor, $\text{CF}_0\text{--CF}_1$. A similar mode of action has been reported, for instance, in the case of natural phytotoxins, such as euparin, a phytotoxic substance isolated from *Helianthella quinquerensis*,⁴⁸ and chalepensis, a coumarin isolated from *Stauranthus perforatus*,⁴⁹ and synthetic analogues of natural compounds.⁵⁰ To support this hypothesis, the effect of the most active compound, 11, was evaluated also under uncoupling conditions. Indeed, results (Figure 4) clearly showed that it influences the basal electron flow without

affecting the uncoupled rate. On the contrary, the inhibition exerted by compounds **7** and **8** was evident under both conditions (data not shown).

Regardless of the mechanism, substances able to interfere with the photosynthetic electron transport chain are potentially susceptible to be endowed with biological activity against photosynthetic organisms. However, this is not obvious, because several factors, including differential membrane permeability/solubility, subcellular compartmentalization, and the occurrence of metabolism/detoxification reactions, can completely abolish inside the cell the inhibitory potential found *in vitro* for a given compound. To verify such a possibility, some of the analogues that had previously shown efficacy *in vitro* were characterized with respect to their ability to inhibit the photoautotrophic growth of a model strain of the blue-green alga *Synechococcus*. Results, summarized in Figure 5, showed that compounds **10**, **11**, **12**, and **13** were actually able to significantly reduce cell proliferation at micromolar levels.

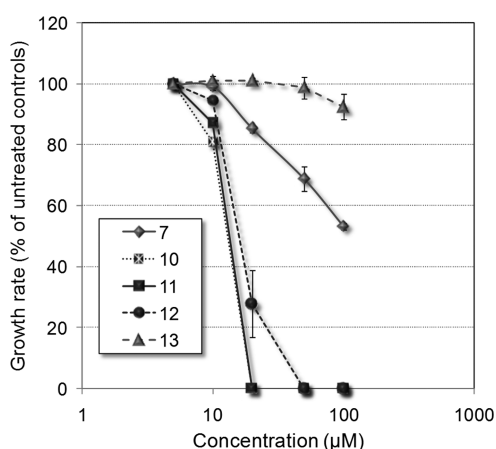


Figure 5. Effects of selected isobenzofuran-1(3H)-ones on the growth of the cyanobacterium *Synechococcus elongatus*. Its growth constant under photoautotrophic conditions was measured in Bg11 medium and in media containing increasing concentrations of cryphonectric acid analogues. Results were expressed as percent of untreated controls and are means \pm SE over four independent replicates. Data were subjected to analysis of variance: with the only exception of compound **7**, all tested isobenzofuran-1(3H)-ones significantly ($P < 0.001$) lowered algal growth rate at 20 μ M.

Interestingly, the relative effectiveness of these compounds strictly reflected that found *in vitro* against the electron transport chain, since the three analogues acting as uncouplers (**10**, **11**, and **12**) were significantly more effective than those (**7** and **13**) affecting both the basal and the uncoupled rate. In the case of compounds **10** and **11**, cyanobacterial growth was completely abolished at a concentration as low as 20 μ M. Although indirect, such evidence seems thus to support the possibility that these cryphonectric acid analogues may be able to interfere with the photosynthetic electron transport chain *in vivo*, therefore exerting phytotoxic effects.

Structure–Activity Relationship Analysis. Bioactive compounds have to cross several barriers to reach their target sites. Their availability in a biological system (bioavailability) depends upon several parameters, such as solubility, membrane permeability, and active uptake and transport within the organism.⁵¹

Lipinski and colleagues defined properties and molecular features that are typically associated with orally active drugs in

humans and summarized them in the “rule-of-five”.³⁸ Veber and co-workers added a few more related criteria.⁵² However, these parameters do not apply to compounds that are used as pesticides.

Bioavailability of compounds in plants is an important parameter in chemical genetics.⁵³ Tice analyzed the molecular properties of herbicides, resulting in “Tice’s rule-of-five”, which is strikingly similar to Lipinski’s rule (Table 2).⁵⁴ Tice’s rule can be used to predict the bioavailability of small molecules in plants.

Table 2. Reference Values of the Rules of Lipinski, Veber, and Tice

compd	cLogP	MW	PSA	HBD	HBA	nRotB
Lipinski ^a	≤ 5	≤ 500		≤ 5	≤ 10	
Veber ^b			≤ 140			≤ 10
Tice ^c	≤ 5	150–500	50–60	≤ 3	2–12	≤ 12

^aLipinski’s rule-of-five for pharmaceuticals. ^bVeber added more criteria to Lipinski’s rule-of-five. ^cTice’s modified rule-of-five for postemergence herbicides.

Considering the results of *in vivo* and *in vitro* biological assays described above, a computational study was carried out to predict the physicochemical parameters of compounds **3–13** and verify if the substances can fulfill Tice’s rule-of-five for herbicides. These parameters (Table 3) were calculated by using Molinspiration (<http://www.molinspiration.com/cgi-bin/properties>), a free computational tool that helps to predict properties of compounds.^{55,56}

Tice’s rule-of-five used Ghose and Crippen’s aLogP to describe the bioavailability of herbicides.⁵⁷ However, aLogP values are comparable to Lipinski’s calculated LogP (cLogP) values presented in Table 3 ($a\text{LogP} \approx c\text{LogP}$). As can be seen, none of the compounds violates Tice’s rule concerning LogP criteria. We could not find any plain correlation between cLogP values and the investigated biological activities of compounds **3–13**. For the most active inhibitors of *S. elongatus* cell proliferation, cLogP values were within the range of 2.183–4.480.

With the exception of PSA, all compounds exhibited physicochemical parameter values within the limits proposed by Tice (Table 3). In his study, it was found that the average molecular weight for commercial herbicides is 329. The three most active compounds inhibiting *S. elongatus* growth, **10–12**, have values close to this average. With respect to the PSA, all compounds violate Tice’s rules. Whereas chemicals **3–10** exhibit PSA values slightly higher compared to Tice’s range, PSA values for compounds **11–13** are completely outside it. However, several examples of commercial herbicides that violate this criteria are known.⁵⁴

Hydrogen-bonding capacity (the number of HBA) was estimated by considering the number of nitrogen and oxygen atoms in the chemical structure.⁵⁸ The number of HBD atoms corresponds to the sum of hydrogen atoms bound to oxygen and to nitrogen atoms. Among the herbicides currently in use, 93% have been shown to have two or fewer hydrogen-bond donors.⁵⁴ This feature is presented by the most active compounds **10–12**, which have two hydrogen-bond donors. It is worth mentioning that considering the proposed limits by Tice for HBA and HBD (Table 3), none of the evaluated compounds violate them.

Table 3. Predicted Physicochemical Properties of Compounds 3–13

compd	cLogP ^a	MW ^b	PSA ^c	HBD ^d	HBA ^e	nRotB	volume
3	1.741	244.0	63.604	1	4	1	211.979
4	1.982	258.0	63.604	1	4	1	228.566
5	3.483	286.0	63.604	1	4	2	261.955
6	2.394	272.0	63.604	1	4	1	244.803
7	0.652	278.0	60.447	0	4	1	195.554
8	3.016	242.0	66.761	2	4	1	205.442
9	3.416	256.0	66.761	2	4	1	222.003
10	4.480	284.0	66.761	2	4	2	255.392
11	2.183	326.0	100.903	2	6	3	243.409
12	2.584	340.0	100.903	2	6	3	259.970
13	3.647	368.0	100.903	2	6	4	293.359

^acLogP, calculated lipophilicity. ^bMW, molecular weight. ^cPSA, polar surface area. ^dHBD, number of hydrogen bond donor. ^eHBA, number of hydrogen bond acceptor.

The number of rotatable bonds is a simple topological parameter of molecular flexibility. Chemicals 3–13 do not violate Tice's rules concerning this parameter. Once again, no plain correlation was observed between this parameter and biological activity, 11, 12, and 13 being the compounds with higher flexibility among the evaluated substances with nRotB equal to 3, 3, and 4, respectively (Table 3).

The molecular volume can be used as a measurement of molecular similarity and can help in understanding the steric requirements of a receptor. Looking at Table 3, it can be noted that the calculated molecular volumes for compounds 5, 6, and 10–12 are similar. Compounds 5 and 6 are completely inactive on the photosynthetic apparatus and have alicyclic groups attached to the C-3 position of the isobenzofuranone unit. Substances 10–12 act as uncouplers and present an aromatic ring attached to the C-3 position. These facts suggest that the presence of an aromatic ring has a beneficial effect in terms of uncoupler activity of the isobenzofuranones herein investigated. The effect of the most active compounds on the growth of the blue-green alga could be correlated with molecular volume. These data fitted a second-order polynomial function, in which the variation of the phytotoxic effect with molecular volume is clearly shown (Figure 6).

We also investigated possible correlations between biological activity, energies of LUMO–HOMO, and dipole moments. The energy gap between the highest occupied molecular orbital (HOMO) and the lowest unoccupied molecular orbital

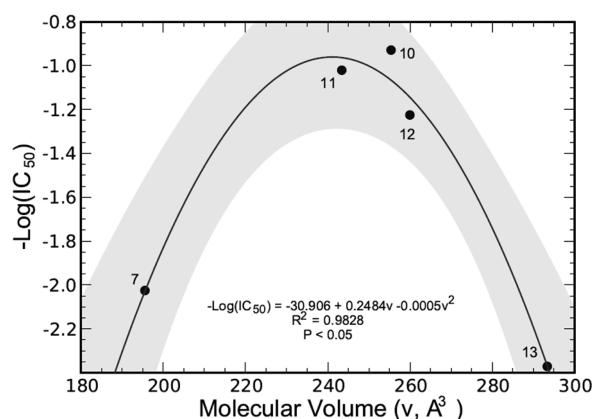


Figure 6. Phytotoxicity against the blue-green alga *Synechococcus* versus molecular volume for compounds 7 and 10–13. The shaded region corresponds to a confidence interval of 95%.

(LUMO) ($\epsilon\text{LUMO} - \epsilon\text{HOMO}$) is related to the chemical stability of a compound. A large value of this descriptor is considered to be an indicator of a higher stability of the compound toward chemical reactions.⁵⁹ A clear correlation of biological activity with the measures of nucleophilicity and electrophilicity (HOMO and LUMO, respectively) was not evident (Table 4).

Table 4. Quantum-Chemical Descriptors

compd	HOMO	LUMO	GAP _(HOMO–LUMO)	dipole moment
3	−6.79	−1.81	4.98	5.11
4	−6.75	−1.81	4.94	5.32
5	−6.72	−1.81	4.91	5.10
6	−6.77	−1.81	4.96	5.11
7	−7.21	−2.54	4.67	6.35
8	−6.23	−1.80	4.43	5.10
9	−6.18	−1.80	4.38	9.23
10	−6.16	−1.79	4.37	9.25
11	−7.07	−1.73	5.34	7.69
12	−7.02	−1.72	5.30	8.39
13	−6.99	−1.72	5.27	8.53

The dipole moment is an important molecular descriptor that gives the measure of bond polarity and charge separation throughout the molecule (Table 4). The biological activity of the compounds able to interfere with the basal rate of the electron transport chain could be correlated with the calculated dipole moment values (Figure 7).

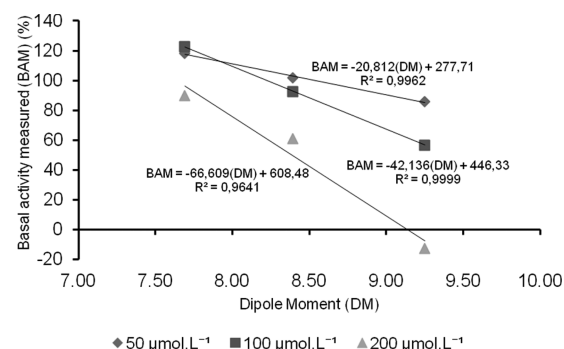


Figure 7. Phytotoxicity (in vitro effects on ferricyanide reduction by functionally intact chloroplasts) versus dipole moment for compounds 10–12.

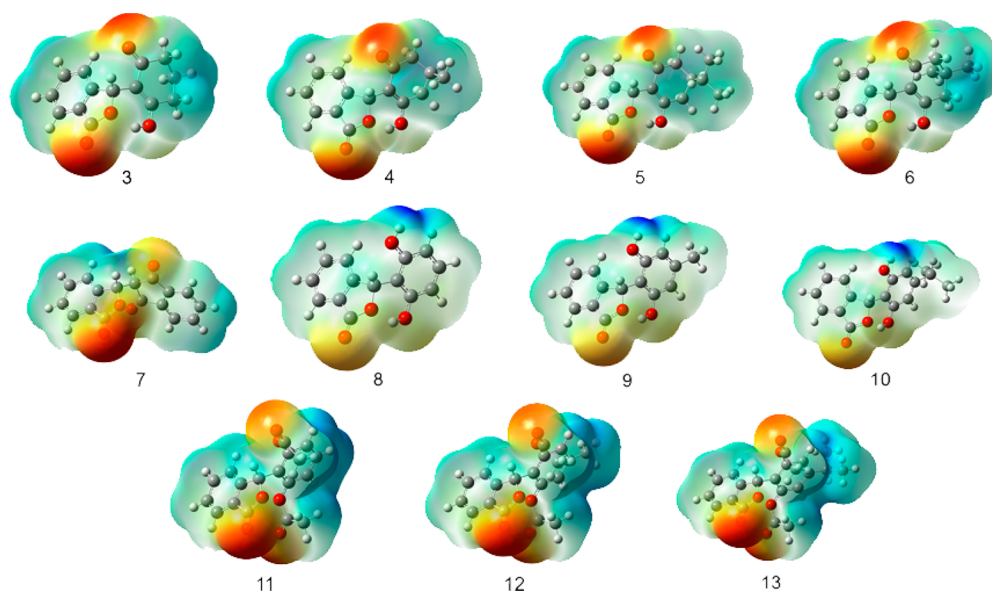


Figure 8. Comparison of the electrostatic potential surfaces of compounds 2–13 from DFT calculations.

The electrostatic potential surfaces of phtalides 3–13 are shown in Figure 8. Comparison of these surfaces did not show any significant difference in charge distribution that could be correlated with the biological profile of the compounds considering either *in vitro* or *in vivo* assays.

In summary, experimental evidence showed that 7 of 11 compounds are able to interfere with the Hill reaction catalyzed by isolated spinach chloroplasts. Three of them at high concentrations inhibited both the basal and the uncoupled rate, suggesting an interaction with the photosynthetic apparatus at the level of the electron transport chain. On the contrary, another four substances acted as uncouplers, showing a much higher effectiveness. Consistent with previous results on other synthetic analogues of natural phytotoxins, the nostocides,⁴³ these data suggest that even small changes in the chemical structure of a scaffold can lead to significant changes in the mode of interaction with the chloroplastic machinery. Although less effective than some commercial herbicides targeting photosynthesis,³⁶ micromolar levels of the most active cryphonectric acid derivatives were able to completely suppress the photoautotrophic growth of a model cyanobacterial strain. They may thus represent a novel scaffold to be exploited aiming at the development of new active ingredients for weed control.

■ ASSOCIATED CONTENT

Ⓢ Supporting Information

Coordinates of the lowest energy conformers for compounds 3–13 and energy maps of the highest occupied molecular orbital (E_{HOMO}) and lowest unoccupied molecular orbital (E_{LUMO}) of cryphonectric acid analogues. This material is available free of charge via the Internet at <http://pubs.acs.org>.

■ AUTHOR INFORMATION

Corresponding Author

*(R.R.T.) Phone: (55) 31 3899 3209. E-mail: robsonr.teixeira@ufv.br. (G.F.) Phone: (39) 0532 45 5311. E-mail: flg@unife.it.

Funding

We are grateful to the following Brazilian agencies: Conselho Nacional de Desenvolvimento Científico e Tecnológico (CNPq) and Coordenação de Aperfeiçoamento de Pessoal de Nível Superior (CAPES) for research fellowships; Fundação de Amparo a Pesquisa de Minas Gerais (FAPEMIG) for a research grant (R.R.T.) and research fellowship (F.M.O.). Partial support from the University of Ferrara (Fondo di Ateneo per la Ricerca 2011) is also acknowledged.

Notes

The authors declare no competing financial interest.

■ ACKNOWLEDGMENTS

The skillful technical assistance of Daniele Faccini is acknowledged.

■ REFERENCES

- (1) Wiebe, K. How to feed the world in 2050. OECD Global Forum on Agriculture. [online]; available at <http://www.oecd.org/dataoecd/43/6/43256458.pdf> (accessed Dec 30, 2012).
- (2) Tomlin, C. D. S. *The Pesticide Manual*, 14th ed.; BCPC: Alton, UK, 2006.
- (3) Böger, P.; Wakabayashi, K.; Hirai, K. *Herbicide Classes in Development. Mode of Action, Targets, Genetic Engineering, Chemistry*; Springer-Verlag: Berlin, Germany, 2002.
- (4) Ware, G. W. *The Pesticide Book*, 5th ed.; Thomson Publications: Fresno, CA, 2000; pp 109–132.
- (5) Gressel, J. Evolving understanding of the evolution of herbicide resistance. *Pest Manag. Sci.* **2009**, *65*, 1164–1173.
- (6) Vencil, W.; Grey, T.; Culpepper, S. Resistance of weeds to herbicides. In *Herbicides and Environment*; Kortekamp, A., Ed.; In Tech: Croatia, 2011; pp 585–594.
- (7) Shaner, D. L.; Lindenmeyer, R. B.; Ostlie, M. H. What have the mechanisms of resistance to glyphosate taught us? *Pest Manag. Sci.* **2012**, *68*, 3–9.
- (8) Heap, I. International Survey of Herbicide Resistant Weeds [online]; available at <http://www.weedscience.org> (accessed Dec 30, 2012).
- (9) Godfrey, C. R. A. *Agrochemicals from Natural Products*; Dekker: New York, 1995.

- (10) Copping, L. G. *Crop Protection Agents from Nature. Natural Products and Analogues*; The Royal Society of Chemistry: London, UK, 1996.
- (11) Duke, S. O.; Dayan, F. E.; Romagni, J. G.; Rimando, A. M. Natural products as sources of herbicides: current status and future trends. *Weed Res.* **2000**, *40*, 99–111.
- (12) Duke, S. O.; Dayan, F. E.; Rimando, A. M.; Schrader, K. K.; Aliotta, G.; Oliva, A.; Romagni, J. G. Chemicals from nature for weed management. *Weed Sci.* **2002**, *50*, 138–151.
- (13) Barbosa, L. C. A.; Teixeira, R. R.; Montanari, R. M. Phytotoxic natural products as models for the development of crop protection agents. In *Current Trends in Phytochemistry*; Epifano, F., Ed.; Research Signpost: Kerala, India, 2008; pp 21–59.
- (14) Dayan, F. E.; Cantrell, C. L.; Duke, S. O. Natural products in crop protection. *Bioorg. Med. Chem.* **2009**, *17*, 4022–4034.
- (15) Duke, S. O.; Cantrell, C. L.; Meepagala, K. M.; Wedge, D. E.; Tabanca, N.; Schrader, K. K. Natural toxins for use in pest management. *Toxins* **2010**, *2*, 1943–1962.
- (16) Scharader, K. K.; Andolfi, A.; Cantrell, C. L.; Cimmino, A.; Duke, S. O.; Osbrink, W.; Wedge, D. E.; Evidente, A. A survey of phytotoxic microbial and plant metabolites as potential natural products for pest management. *Chem. Biodiversity* **2010**, *7*, 2261–2280.
- (17) Hüter, O. F. Use of natural products in the crop protection industry. *Phytochem. Rev.* **2011**, *10*, 185–194.
- (18) Cantrell, C. L.; Dayan, F. E.; Duke, S. O. Natural products as sources for new pesticides. *J. Nat. Prod.* **2012**, *75*, 1231–1242.
- (19) Saxena, S.; Pandey, A. K. Microbial metabolites as eco-friendly agrochemicals for the next millennium. *Appl. Microbiol. Biotechnol.* **2001**, *55*, 395–403.
- (20) Copping, L. G.; Duke, S. O. Natural products that have been used commercially as crop protection agents. *Pest Manag. Sci.* **2007**, *63*, 524–554.
- (21) Beaudagnies, R.; Edmunds, A. J. F.; Fraser, T. E. M.; Hall, R. G.; Hawkes, T. R.; Mitchell, G.; Schaetzler, J.; Wendeborn, S.; Wibley, J. Herbicidal 4-hydroxyphenylpyruvate dioxygenase inhibitors – a review of the triketone chemistry story from a Syngenta perspective. *Bioorg. Med. Chem.* **2009**, *17*, 4134–4152.
- (22) Wu, N. Herbicide sulcotrione. In *Herbicides, Theory and Applications*; Soloneski, S.; Larramendy, M. L., Eds.; In Tech: Croatia, 2011; pp 527–544.
- (23) Logrado, L. P. L.; Santos, C. O.; Romeiro, L. A. S.; Costa, A. M.; Ferreira, J. R. O.; Cavalcanti, B. C.; de Moraes, M. O.; Costa-Lotuf, L. V.; Pessoa, C.; Dos Santos, M. L. Synthesis and cytotoxicity screening of substituted isobenzofuranones designed from anacardic acids. *Eur. J. Med. Chem.* **2010**, *45*, 3480–3489.
- (24) Ygonathan, K.; Rossant, C.; Ng, S.; Huang, Y.; Butler, M. S.; Buss, A. D. 10-Methoxydihydrofusicin, fusicinarin and fusicin, novel antagonists of the human CCR5 receptor from *Oidiodendron griseum*. *J. Nat. Prod.* **2003**, *66*, 1116–1117.
- (25) Cardozo, J. A.; Braz-Filho, R.; Rincón-Velandia, J.; Guerrero-Pabón, M. F. 3-Butyl-isobenzofuranona: un compuesto aislado de *Apium graveolens* con actividad anticonvulsivante. *Rev. Col. Cienc. Quim. Farm.* **2005**, *34*, 69–76.
- (26) Huang, X.-Z.; Zhu, Y.; Guan, X.-L.; Tian, K.; Guo, J.-M.; Wang, H.-B.; Fu, G.-M. A novel antioxidant isobenzofuranone derivative from fungus *Cephalosporium* sp. AL031. *Molecules* **2012**, *17*, 4219–4224.
- (27) Ma, F.; Gao, Y.; Qiao, H.; Hu, X.; Chang, J. Antiplatelet activity of 3-butyl-6-bromo-1(3H)-isobenzofuranone on rat platelet aggregation. *J. Thromb. Thrombolysis* **2012**, *33*, 64–73.
- (28) Demuner, A. J.; Barbosa, L. C. A.; Veiga, T. A. M.; Barreto, R. W.; King-Diaz, B.; Lotina-Hennsen, B. Phytotoxic constituents from *Nimbya alternantherae*. *Biochem. Syst. Ecol.* **2006**, *34*, 790–795.
- (29) Mal, D.; Pahari, P. Recent advances in the Hauser annulation. *Chem. Rev.* **2007**, 1892–1918.
- (30) Egan, B. A.; Paradowski, M.; Thomas, L. H.; Marquez, R. Regiocontrolled rearrangements of isobenzofurans. *Org. Lett.* **2011**, *13*, 2086–2089.
- (31) Arnone, A.; Assante, G.; Nasini, G.; Strada, S.; Vercesi, A. Cryphonectric acid and other metabolites from a hypovirulent strain of *Cryphonectria parasitica*. *J. Nat. Prod.* **2002**, *65*, 48–50.
- (32) Barbosa, L. C. A.; Rocha, M. E.; Teixeira, R. R.; Maltha, C. R. A.; Forlani, G. Synthesis of 3-(4-bromobenzyl)-5-(arylmethylene)-5H-furan-2-ones and their activity as inhibitors of the photosynthetic electron transport chain. *J. Agric. Food Chem.* **2007**, *55*, 8562–8569.
- (33) Teixeira, R. R.; Barbosa, L. C. A.; Forlani, G.; Piló-Veloso, D.; Carneiro, J. W. de M. Synthesis of photosynthesis-inhibiting nostoclide analogues. *J. Agric. Food Chem.* **2008**, *56*, 2321–2329.
- (34) Barbosa, L. C. A.; Nogueira, L. B.; Maltha, C. R. A.; Teixeira, R. R.; Silva, A. A. Synthesis and phytochemical properties of oxabicyclic analogues related to helminthosporin. *Molecules* **2009**, *14*, 160–173.
- (35) Barbosa, L. C. A.; Demuner, A. J.; Maltha, C. R. A.; Teixeira, R. R.; Souza, K. A. P.; Bicalho, K. A. Phytochemical activity of 3-(3-chlorobenzyl)-5-arylidene-furan-2(5H)-ones. *Z. Naturforsch.* **2009**, *64B*, 245–251.
- (36) Vicentini, C. B.; Mares, D.; Tartari, A.; Manfrini, M.; Forlani, G. Synthesis of pyrazole derivatives and their evaluation as photosynthetic electron transport inhibitors. *J. Agric. Food Chem.* **2004**, *52*, 1898–1906.
- (37) Lichtenthaler, H. K. Chlorophylls and carotenoids: pigments of photosynthetic biomembranes. *Methods Enzymol.* **1987**, *148*, 350–382.
- (38) Lipinski, C. A.; Lombardo, F.; Dominy, B. W.; Feeney, P. J. Experimental and computational approaches to estimate solubility and permeability in drug discovery and development settings. *Adv. Drug Delivery Rev.* **1997**, *23*, 3–25.
- (39) Ertl, P.; Rohde, B.; Selzer, P. Fast calculation of molecular polar surface area as a sum of fragment-based contributions and its application to the prediction of drug transport properties. *J. Med. Chem.* **2000**, *43*, 3714–3717.
- (40) Spartan 10, 1.2.0, Wavefunction, Inc., Irvine, CA. For a description of the improved calculation of ¹³C-NMR chemical shifts in Spartan 10 see: *Spartan '10 for Windows, Macintosh and Linux – Tutorial and User's Guide*; Wavefunction, Inc.: Irvine, CA, 2011; pp 480–487.
- (41) Frisch, M. J.; Trucks, G. W.; Schlegel, H. B.; Scuseria, G. E.; Robb, M. A.; Cheeseman, J. R.; Scalmani, G.; Barone, V.; Mennucci, B.; Petersson, G. A.; Nakatsuji, H.; Caricato, M.; Li, X.; Hratchian, H. P.; Izmaylov, A. F.; Bloino, J.; Zheng, G.; Sonnenberg, J. L.; Hada, M.; Ehara, M.; Toyota, K.; Fukuda, R.; Hasegawa, J.; Ishida, M.; Nakajima, T.; Honda, Y.; Kitao, O.; Nakai, H.; Vreven, T.; Montgomery, J. A., Jr.; Peralta, J. E.; Ogliaro, F.; Bearpark, M.; Heyd, J. J.; Brothers, E.; Kudin, K. N.; Staroverov, V. N.; Kobayashi, R.; Normand, J.; Raghavachari, K.; Rendell, A.; Burant, J. C.; Iyengar, S. S.; Tomasi, J.; Cossi, M.; Rega, N.; Millam, J. M.; Klene, M.; Knox, J. E.; Cross, J. B.; Bakken, V.; Adamo, C.; Jaramillo, J.; Gomperts, R.; Stratmann, R. E.; Yazyev, O.; Austin, A. J.; Cammi, R.; Pomelli, C.; Ochterski, J. W.; Martin, R. L.; Morokuma, K.; Zakrzewski, V. G.; Voth, G. A.; Salvador, P.; Dannenberg, J. J.; Dapprich, S.; Daniels, A. D.; Farkas, Ö.; Foresman, J. B.; Ortiz, J. V.; Cioslowski, J.; Fox, D. J. *Gaussian '09*, revision A.1; Gaussian, Inc.: Wallingford, CT, 2009.
- (42) Becker, A. D. Density-functional thermochemistry. III. The role of exact exchange. *J. Chem. Phys.* **1993**, *98*, 5648–5653.
- (43) Zhang, G.; Musgrave, C. B. Comparison of DFT methods for molecular orbital eigenvalue calculations. *J. Phys. Chem. A* **2007**, *111*, 1554–1561.
- (44) Marenich, A. V.; Cramer, C. J.; Truhlar, D. G. Universal solvation model based on solute electron density and on a continuum model of the solvent defined by the bulk dielectric constant and atomic surface tensions. *J. Phys. Chem. B* **2009**, *113*, 6378–6396.
- (45) Pahari, P.; Senapati, B.; Mal, D. Regiospecific synthesis of isopestacin, a naturally occurring isobenzofuranone antioxidant. *Tetrahedron Lett.* **2004**, *45*, 5109–5112.
- (46) Mal, D.; Pahari, P.; De, S. R. Regiospecific synthesis of 3-(2,6-dihydroxyphenyl) pthalides: application to the synthesis of isopestacin and cryphonectric acid. *Tetrahedron* **2007**, *63*, 11781–11792.
- (47) Oliver, J. E.; Wilzer, K. R.; Waters, R. M. Synthesis of 1-(2,6-dihydroxyphenyl)-1-alkanones and benzophenone by aromatization of

2-acyl-3-hydroxy-2-cyclohexene-1-ones with mercuric acetate. *Synthesis* **1990**, 1117–1119.

(48) Castaneda, P.; Mata, R.; Lotina-Hennsen, B. Effect of enecalinal, euparin and demethylencecalinal on thylakoid electron transport and photophosphorylation in isolated spinach chloroplasts. *J. Sci. Food Agric.* **1998**, *78*, 102–108.

(49) Macias, M. L.; Rojas, I. S.; Mata, R.; Lotina-Hennsen, B. Effect of selected coumarins on spinach chloroplast photosynthesis. *J. Agric. Food Chem.* **1999**, *47*, 2137–2140.

(50) Barbosa, L. C. A.; Varejão, J. O. S.; Petrollino, D.; Pinheiro, P. F.; Demuner, A. J.; Maltha, C. R. A.; Forlani, G. Tailoring nostoclide structure to target the chloroplastic electron transport chain. *Arkivoc* **2012**, *iv*, 15–32.

(51) Lipinski, C. A.; Lombardo, F.; Dominy, B. W.; Feeney, P. J. Experimental and computational approaches to estimate solubility and permeability in drug discovery and development settings. *Adv. Drug Delivery Rev.* **2001**, *46*, 3–26.

(52) Veber, D. F.; Johnson, S. R.; Cheng, H.-Y.; Smith, B. R.; Ward, K. W.; Kopple, K. D. Molecular properties that influence the oral bioavailability of drug candidates. *J. Med. Chem.* **2002**, *45*, 2615–2623.

(53) Tóth, R.; van der Hoorn, R. A. L. Emerging principles in plant chemical genetics. *Trends Plant Sci.* **2010**, *15*, 81–88.

(54) Tice, C. M. Selecting the right compounds for screening: does Lipinski's Rule of 5 for pharmaceuticals apply to agrochemicals? *Pest Manag. Sci.* **2001**, *57*, 3–16.

(55) Haines, D. S.; Burnell, J. N.; Doyle, J. R.; Llewellyn, L. E.; Motti, C. A.; Tapiolas, D. M. Translation of in vitro inhibition by marine natural products of the C4 acid cycle enzyme pyruvate Pi dikinase to in vivo C4 plant tissue death. *J. Agric. Food Chem.* **2005**, *53*, 3856–3862.

(56) Hu, D.-J.; Liu, S.-F.; Huang, T.-H.; Tu, H.-Y.; Zhang, A.-D. Synthesis and herbicidal activities of novel 4-(4-(5-methyl-3-arylisoaxazol-4-yl)thiazol-2-yl)piperidyl carboxamides and thiocarboxamides. *Molecules* **2009**, *14*, 1288–1303.

(57) Ghose, A. K.; Crippen, G. M. Atomic physicochemical parameters for three dimensional structure-directed quantitative structure-activity relationships. I. Partition coefficients measure of hydrophobicity. *J. Comput. Chem.* **1986**, *7*, 565–577.

(58) Lipinski, C. A. Lead- and drug-like compounds: the rule-of-five revolution. *Drug Discov. Today Technol.* **2004**, *1*, 337–341.

(59) Wang, Z.; Song, J.; Han, Z.; Jiang, Z.; Zheng, W.; Chen, J.; Song, Z.; Shang, S. Quantitative structure-activity relationship of terpenoid aphid antifeedants. *J. Agric. Food Chem.* **2008**, *56*, 11361–11366.